A Molecular Dynamics Simulation Study of Segmental Relaxation Processes in Miscible Polymer Blends

Dmitry Bedrov* and Grant D. Smith

Department of Materials Science and Engineering, University of Utah, 122 S. Central Campus Dr., Rm. 304, Salt Lake City, Utah 84112

Received April 19, 2006; Revised Manuscript Received September 19, 2006

ABSTRACT: We have performed molecular dynamics simulations of blends composed of chemically realistic (CR) and lower barrier (LB) 1,4-polybutadiene (PBD) over a wide range of composition and temperature. In these blends, the dynamically fast component (LB-PBD, $T_g \approx 108$ K) and dynamically slow component (CR-PBD, $T_g \approx 164$ K) are conformationally, structurally, and thermodynamically very similar, with different dihedral barriers leading to significantly different segmental dynamics. We observe primary (α-relaxation) and secondary main-chain (β-relaxation) processes in the dielectric response of pure melts and CR-PBD/LB-PBD blends for all temperatures and compositions investigated. The separation between the dielectric α- and β-relaxation processes of the fast component polymer significantly increases upon blending. This increasing separation dramatically influences the frequency-dependent dielectric susceptibility of the blend due to the significant strength of the fast component β-relaxation process and the insensitivity of this relaxation process to the blend composition, providing a plausible explanation for the broadening of the blend dielectric response observed experimentally in a number of miscible blends. The results obtained from our simulations are discussed in light of concentration fluctuation, Lodge−McLeish, and coupling models.

I. Introduction

Understanding the influence of blending on mechanisms of segmental relaxation is a crucial step in our ability to tailor dynamical and viscoelastic properties of polymer mixtures and has been a focus of numerous experimental and theoretical studies.[1] Much of this effort has involved application of NMR relaxation, dielectric spectroscopy, and QENS measurements to polymer blends of components with various degrees of thermodynamic compatibility, structural similarity, and dynamic asymmetry. One of the remarkable and almost universal characteristics of miscible polymer blends is the distinct segmental dynamics of the component polymers. Specifically, the component polymers of miscible blends exhibit segmental relaxation times that differ in magnitude and temperature dependence from each other and from their corresponding pure melt values. Preservation of the individual character in the segmental dynamics of each blend component instead of following some average (defined by blend composition) segmental dynamics has inspired development of theoretical models that attempt to provide mechanistic insight into as well as predictive descriptions of this phenomenon.

Theoretical models have been suggested to explain dynamical behavior of blends and their components based on thermally driven concentration fluctuations,[2] chain connectivity,[3] or a combination of both.[4−6] In these models, the segmental dynamics of a polymer are thought to be determined by the local environment that can deviate from the average blend composition. The Lodge−McLeish (LM) model[3] suggests that segmental dynamics are determined by the environment on the scale of the polymer statistical segment defined by the Kuhn length l_K. On this length scale, chain connectivity results in a local environment for a polymer segment that is richer in segments of its own type than the average blend composition. The effective local concentration around a segment can be defined as

$$\phi_{\text{eff}} = \phi_{\text{self}} + (1 - \phi_{\text{self}})\phi \tag{1}$$

where ϕ is the blend composition (volume fraction of A or B segments) and ϕ_{self} is the so-called "self-concentration" of the component under consideration (A or B) and corresponds to the volume fraction occupied by a polymer segment in the volume $V \sim l_K^3$. The model correlates ϕ_{eff} with a glass transition temperature $T_{g,\text{eff}}(\phi)$ for the local environment (quantified by ϕ_{eff}) of polymer segment, which is assumed to be equal to $T_g(\phi_{\text{eff}})$. To predict $T_g(\phi_{\text{eff}})$ the glass transition temperature of the pure components (T_g^A and T_g^B) can be used, assuming that a mixing rule such as the Fox equation[7]

$$\frac{1}{T_{g,\text{eff}}(\phi)} = \frac{1}{T_g(\phi_{\text{eff}})} = \frac{\phi_{\text{eff}}^A}{T_g^A} + \frac{1 - \phi_{\text{eff}}^A}{T_g^B} \tag{2}$$

is applicable. Here ϕ_{eff}^A and ϕ_{eff}^B are the effective (local) concentrations (from eq 1) of A and B segments around the segment of interest. The LM model assumes that the segmental relaxation of the components in the blend is qualitatively (mechanistically) the same as in pure melts of components and that only their temperature dependence shifts upon blending. If the segmental relaxation of a pure melt of the component A can be described by a Vogel−Fulcher (VF) temperature dependence[8,9]

$$\tau_{\text{seg}}^A(T) = \tau_\infty^A \exp\left[\frac{B^A}{T - T_0^A}\right] \tag{3}$$

then the temperature dependence of the segmental relaxation of this component in the blend can be represented by the same VF equation but with a concentration-dependent T_0^A parameter determined as

* Corresponding author. E-mail: bedrov@cluster2.mse.utah.edu.

10.1021/ma0608828 CCC: $33.50
Published on Web 11/04/2006

$$T_0^A(\phi) = T_0^A + (T_g^A(\phi_{eff}) - T_g^A) \quad (4)$$

where T_g^A and $T_g^A(\phi_{eff})$ are the (known) glass transition temperature of the pure melt of polymer A and the (estimated using eq 2) glass transition temperature for the segmental relaxation of an A segment in the blend, respectively.

Another class of models[2,4−6] assumes that segmental dynamics are determined by a local region that can be spontaneously rich in segments of either blend component due to thermal concentration fluctuations (CF) in addition to a chain connectivity effect discussed above. It is assumed that these fluctuations are Gaussian distributed

$$P(\phi_{eff}) \propto \exp\left[-0.5\frac{(\phi_{eff} - \langle\phi_{eff}\rangle)^2}{\langle(\delta\phi_{eff})^2\rangle}\right] \quad (5)$$

about some average effective concentration ϕ_{eff} with $\langle(\delta\phi_{eff})^2\rangle$ variance. The size of this local region is related to cooperatively rearranging volumes associated with the glass transition[10] and (depending on the particular variation of the CF model) has certain temperature and composition dependences. According to these models, a segment of each component can have a broad distribution of local environments ranging from pure melt-like to dilute limits on length scales of several nanometers that consequently leads to a broad distribution of segmental relaxation times $P(\tau_{seg})$ of the components and the blend. Similar to the LM model, the effective T_g for each component in the blend as a function of ϕ_{eff} can be estimated using data for the pure melts of the components while the dynamical response of each component in the blend as well as total of the blend can be predicted taking into account the assumed distributions of local environments $P(\phi_{eff})$ and the corresponding distributions of the segmental relaxations $P(\tau_{seg})$.

Both the LM and CF models attempt to account for the influence of the local environment on the segmental relaxation of the component polymers of a blend by assuming that segmental relaxation of components in the blend is qualitatively (mechanistically) the same as in the pure melts of these components and that only relaxation times (or glass transition temperatures) are shifted upon blending. While it has been shown that these models can quantitatively reproduce the composition and temperature dependence of segmental relaxation times for some miscible polymer blends,[11,12] there is a number of blends in which these models are able to predict only qualitative trends observed in experiments or fail completely, indicating that some physics of segmental relaxation in polymers blends is not being captured by these models. Particularly challenging for these models is the prediction of segmental relaxation of the lower T_g (dynamically fast) component of blends consisting of component polymers with very different T_g in the neat melt. For example, the reported apparent weak composition dependence of the poly(ethylene oxide) segmental relaxations in poly(ethylene oxide)/poly(methyl methacrylate) blends measured by the spin−lattice NMR cannot be satisfactory described by the LM model.[13] The LM model also failed to describe segmental dynamics obtained from dielectric spectroscopy measurements in poly(vinyl methyl ether)/polystyrene (PVME/PS) blend for low concentrations of PVME.[14,15]

Another phenomenological model that has been applied to segmental relaxation in polymer blends (as well as melts) is based on a concept of intermolecular coupling of a relaxing segment with its environment. This coupling model[16] (CM) represents the relaxation time for the α-relaxation process as

$$\tau_\alpha = \tau_0(\tau_0/t_c)^{n/(1-n)} \quad (6)$$

where τ_0 is the primitive relaxation time, t_c is the crossover time (onset of coupling) that has been shown to be around 2 ps for most polymers,[17] and n is the coupling parameter which can be related to the β parameter ($n = 1 - \beta$) of the Kohlrausch−Williams−Watts (KWW) function[18,19] (see below) that describes the α-relaxation process in the time domain. Changes of this coupling parameter as a function of blend composition can effectively reflect broadening of the α-relaxation process due to concentration fluctuations. Recently, it has been suggested that the primitive relaxation time τ_0 in this model can be associated with the Johari−Goldstein (JG) relaxation process (β-relaxation process),[20] therefore defining the separation between the primary (α-relaxation) and secondary (β-relaxation) processes as

$$\log(\tau_\alpha) - \log(\tau_\beta) = n[\log(\tau_\alpha) - \log(t_c)] \quad (7)$$

Since it is frequently observed that the segmental relaxation of a dynamically fast polymer both slows and broadens (i.e., β decreases) upon blending with a dynamically slower component, the CM (eq 7) suggests that the separation between the α- and β-relaxation processes in the fast blend component will increase upon blending. While the CM is the only model for polymer blends (or melts) that we are aware of that attempts to correlate α- and β-relaxation processes, the mechanisms of correlation (or coupling) of segmental dynamics with the surrounding matrix are not rigorously defined, and therefore the composition dependence of the CM parameters and the influence of blending on relaxation times are not predicted within the model. Nevertheless, the CM has been applied to polymer blends[16] and other glass-forming mixtures,[20,21] showing trends qualitatively consistent with experiment, including systems where the LM and CF models have struggled.[22]

Another challenging task for theoretical models is to capture the breadth of the dielectric relaxation experimentally observed for many blends. For example, dielectric measurements on polyisoprene (PI)/poly(vinylethylene) (PVE) blends reveal significant dielectric loss at high frequency that exhibits weak concentration dependence and is located in a frequency range similar to the response of the neat melt of the lower T_g component (PI), as illustrated in Figure 1a.[23] A very recent attempt to apply a CF model for description of the dielectric response of PI/PVE blend[6] resulted in a prediction of a dielectric loss either with qualitatively correct shape (distinct high-frequency wing) but much narrower than observed in experiments or with reasonable broadness but without a high-frequency wing.

It is clear that additional understanding of the underlying mechanisms of segmental relaxation in polymer blends would greatly facilitate further progress in developing models that correlate segmental dynamics with blend structure. Molecular dynamics (MD) simulations, which have already made important contributions to our understanding of segmental dynamics in polymer melts, are in principle a perfect tool to address the issues of segmental relaxation in miscible polymer blends. In this work, we employ MD simulation to investigate the composition and temperature dependence of segmental relaxations in model polymer blends. We then discuss our results in light of the theoretical models discussed above and suggest an alternative explanation for some puzzling dynamical features observed experimentally in polymer blends.

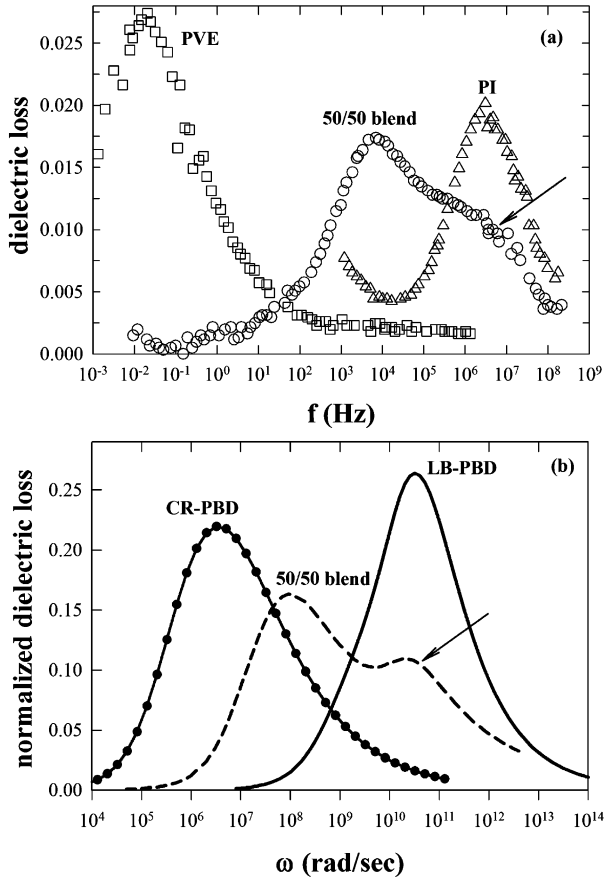

Figure 1. Frequency-dependent dielectric loss of (a) 50/50 PI/PVE blend, PI melt, and PVE melt at 270 K (data from ref 23) and (b) 50/50 LB-PBD/CR-PBD blend, LB-PBD melt, and CR-PBD melt at 198 K obtained from MD simulations. Arrows indicate concentration-independent shoulder at high frequencies.

II. Model Description and Simulation Methodology

In this work, we have significantly extended our investigation of blends comprised of chemically realistic 1,4-polybutadiene (CR-PBD) and lower barrier 1,4-polybutadiene (LB-PBD) chains.[24] CR-PBD is represented using a quantum chemistry based united atom force field[25] that has been extensively validated against NMR spin−lattice relaxation,[26] dynamic neutron scattering,[27] and dielectric relaxation[28] measurements. To create a blend component with faster dynamics, the dihedral barriers of all backbone dihedrals (except double bonds) were reduced by a factor of 4 relative to the CR-PBD model (we refer to this model as low barrier chains or LB-PBD). Figure 2 illustrates the dihedral energy profiles for these models for the backbone $C(sp^2)-C(sp^3)-C(sp^3)-C(sp^2)$ (alkyl) dihedral. All other bonded and nonbonded interactions in the CR-PBD and LB-PBD models are identical. Our previous simulations[29] have already demonstrated that modification of dihedral barriers in PBD melts has little influence on structural but dramatically influences dynamic properties. We illustrated recently that reduction of the dihedral barriers in the LB-PBD melt resulted in significantly lower T_g (108 K) than is observed for the CR-PBD (164 K).[30] Hence, mixing of LB-PBD and CR-PBD chains provides us with a model polymer blend in which the components are quite different dynamically and yet have very similar structure, thermodynamics, and chain conformations.

All blends consisted of 40 chains, each having 30 repeat units. Bonds were constrained using the SHAKE algorithm.[31] A cutoff radius of 10 Å was used for truncation of van der Waals interactions. A multiple time step integrator with 1 fs time step

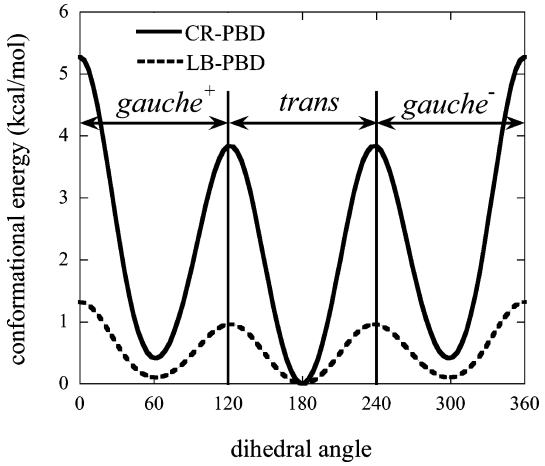

Figure 2. Conformational energy of the $C(sp^2)-C(sp^3)-C(sp^3)-C(sp^2)$ (alkyl) dihedrals as a function of dihedral angle for the CR-PBD and LB-PBD models. Also shown is the division of alkyl dihedral angles into gauche$^+$, trans, and gauche$^-$ conformational states.

for integration of bonded degrees of freedom (bends and torsions) and 5 fs time step for nonbonded (intermolecular and intramolecular separated by five bonds and more) interactions was employed. Original configurations were taken from existing well-equilibrated CR-PBD melts trajectories obtained from our previous simulations. The desired fraction of chains was converted to LB-PBD and subsequently equilibrated over 40 ns followed by production run over 200−800 ns (depending on T and blend composition) using *NVT* ensemble MD simulations. The LB-PBD/CR-PBD blends with 10%, 25%, 50%, and 75% of the LB-PBD have been investigated at 198 K. The LB-PBD/CR-PBD blend with 10% of the LB-PBD has also been investigated as a function temperature at 222, 240, 273, 293, 323, and 400 K, while the LB-PBD/CR-PBD blend with 50% of the LB-PBD has been investigated at 170,180, 222, 240, and 273 K.

III. Analysis of Dipole Relaxation

Dipole relaxation in PBD is due primarily to angular reorientation of the cis H−C═C−H groups that have a net dipole moment (unlike trans H−C═C−H groups, which have no net dipole moment due to symmetry). Since there is no net dipole moment directed along the backbone of the PBD chain, the dipole moment relaxation and dielectric response of PBD is primarily sensitive to segmental motion. Linear response theory allows us to obtain the complex dielectric permittivity $\epsilon(\omega) = \epsilon'(\omega) - i\epsilon''(\omega)$ using the relationship[32]

$$\frac{\epsilon'(\omega) - i\epsilon''(\omega)}{\Delta\epsilon} = 1 - i\omega\int_0^\infty \mathrm{DACF}(t)\exp(-i\omega t)\,\mathrm{d}t \quad (8)$$

where the dipole moment autocorrelation function (DACF) is given as

$$\mathrm{DACF}(t) = \frac{\langle M(0)\cdot M(t)\rangle}{\langle M(0)\cdot M(0)\rangle} = \frac{\sum_{i,j=1}^{N}\langle M_i(0)\cdot M_j(t)\rangle}{\sum_{i,j=1}^{N}\langle M_i(0)\cdot M_j(0)\rangle} \cong \frac{\sum_{i=1}^{N}\langle M_i(0)\cdot M_i(t)\rangle}{\sum_{i=1}^{N}\langle M_i(0)\cdot M_i(0)\rangle} \quad (9)$$

Here $M(t)$ and $M_i(t)$ are the dipole moment of the system (melt

or blend) and the dipole moment of chain i at time t, respectively, and N is the number of chains. For purposes of determining $M(t)$, we assume that the dipole moment of each polymer chain is uncorrelated with that of the other polymer chains, yielding the right-hand expression in eq 9. In calculating the DACF from MD trajectories using eq 9, hydrogen atoms were added to the united atom trajectories in the manner described previously,[33] and partial atomic charges were subsequently assigned to all atoms.[28]

We assume that the contribution of a relaxation process to the (partial) decay of the DACF (eq 9), resulting from segmental motion associated with the relaxation process, can be represented by the Kohlrausch−Williams−Watts (KWW) function[18,19]

$$f(t) = A \exp\left[-\left(\frac{t}{\tau}\right)^{\beta}\right] \tag{10}$$

where τ is the apparent relaxation time, β is the stretching exponent, and A is the amplitude. We represented the autocorrelation functions (eq 9) with the best fit obtainable using a single relaxation process and a sum of two processes, labeled β (short-time) and α (long-time) using

$$\mathrm{DACF}(t) = A_{\beta} f_{\beta}(t) + A_{\alpha} f_{\alpha}(t) \tag{11}$$

Here $f_{\alpha}(t)$ and $f_{\beta}(t)$ are KWW functions (eq 10) representing the α- and β-relaxations, respectively, while A_{α} and A_{β} are amplitudes of these processes with the constraint $A_{\alpha} + A_{\beta} \leq 1.0$. The choice of KWW functions to represent the relaxation processes, as opposed to other functional forms in the time domain, was a matter of convenience. The α-relaxation in polymers is commonly represented with a stretched exponential function in the time domain and an asymmetric (e.g., Havriliak−Negami) function in the frequency domain.[34] The β-relaxation process in polymers, however, is usually considered to be relatively symmetric in the frequency domain and hence is represented with a Cole−Cole function, although asymmetry in the β-relaxation process and the use of a Havriliak−Negami function to represent the process are not unknown.[34] As described below, we find that the β-relaxation process in the LB-PBD melt and LB-PBD component in CR-PBD/LB-PBD blends is typically not very broad; i.e., the stretching exponent β (eq 4) is usually greater than 0.5. A KWW function with $\beta \geq 0.5$ can be represented reasonably well in the frequency domain with a (symmetric) Cole−Cole function.

Relaxation times for the α-relaxation (τ_{α}) and β-relaxation (τ_{β}) processes were determined from the time integral of the corresponding relaxation function, $f_{\alpha}(t)$ and $f_{\beta}(t)$, obtained from fitting and were described by either a Vogel−Fulcher temperature dependence (eq 3) or an Arrhenius temperature dependence

$$\tau(T) = \tau_{\infty} \exp\left(\frac{C}{T}\right) \tag{12}$$

IV. Results and Discussion

A. Segmental Relaxation in the Pure Component Melts. Here we briefly summarize our understanding of segmental relaxation mechanisms in the pure LB-PBD and CR-PBD melts from MD simulations and dielectric relaxation measurements. Detailed study of relaxation mechanisms in the LB-PBD melt[30] has revealed that reduction of dihedral barriers in PBD allows us to observe a clear separation between the α-relaxation process and a low-temperature relaxation process associated with polymer backbone motion, the Johari−Goldstein β-relaxation process.[35] The separation of the α- and β-relaxation processes in the LB-PBD melt can be clearly observed by all probes of segmental relaxation (torsional and dipole moment autocorrelation functions, incoherent dynamic structure factor, C−H vector autocorrelation functions, and dielectric susceptibility) investigated. Mechanistically, we found that the β-relaxation process in LB-PBD melts can be associated with large-scale conformational motions corresponding to all or nearly all dihedrals visiting each conformational state. The β-relaxation process in LB-PBD melts becomes broader and at the same time weaker (in strength) with decreasing temperature due to an increasingly heterogeneous population of conformational states by individual torsions on time scales longer than the β-relaxation time but shorter than the α-relaxation time. This heterogeneity in the population of conformational states is imposed by the matrix which biases conformations of individual dihedrals on time scales shorter than the α-relaxation time and results in an increasing fraction of conformational transitions becoming ineffective in fomenting segmental relaxation with decreasing temperature. Complete segmental relaxation (the α-relaxation process) occurs on longer time scales when a cooperative motion of the matrix results in the breaking up of the segmental cage (due to intermolecular packing), which in turn leads to every dihedral populating each conformational state with near-equilibrium probability.

One of the important conclusions obtained from our investigation of the α- and β-relaxation processes in the LB-PBD melts is that both are operative at all temperatures. Moreover, at high temperatures the β-relaxation process dominates the segmental relaxation. These results are consistent with analysis of the α- and β-relaxation processes in PBD melts from dielectric spectroscopy experiments.[36] It was found that below T_g two loss peaks could be clearly observed, and these were associated with the α- or β-relaxation processes. At temperatures above T_g the dielectric loss exhibits one broad peak which is a combination of contributions from less separated (in frequency) α- and β-relaxation processes. Traditionally, such behavior at higher temperatures is associated with "merging" of α- and β-relaxations into a single process. However, Arbe et al.[36,37] showed that if some characteristics of the α-relaxation process are extrapolated from low temperatures, then the dielectric loss at temperatures above T_g can be fitted with two separate processes (α-relaxation and β-relaxation) that remain separated for all temperatures investigated. They also found that the strength of the α-relaxation process decreases significantly and that β-relaxation process begins to dominate the segmental relaxation with increasing temperature.

At the lowest temperature (198 K) of our simulation of the pure CR-PBD melt, the DACF does not show any obvious signatures of two separated relaxation processes, consistent with the experimentally observed single, broad dielectric loss peak at this temperature.[36] We found that the CR-PBD melt DACF from our MD simulations can be adequately represented by a single ("merged" α- and β-relaxations) KWW process (eq 10) over a wide range of temperatures (198−400 K). However, the stretching exponent β is strongly temperature dependent, which is inconsistent with experimentally observed constant stretching exponent $\beta = 0.41$ for the α-relaxation process in PBD at lower temperatures[36] as well as with the time−temperature superposition principle observed for this system in our previous simulations.[38] This strong temperature dependence of the stretching exponent is indirect evidence that the single "merged" process in reality is a combination of two separate processes that become less separated upon increasing temperature as was suggested by Arbe et al.[36] and in our previous simulation studies of the

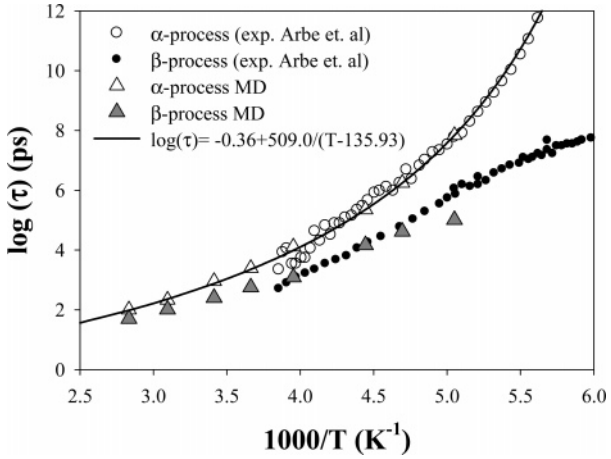

Figure 3. Temperature dependence of the integrated relaxation times of the α- and β-relaxation processes in the CR-PBD melt obtained from fitting DACFs (triangles) and from analysis of experimental data by Arbe et al. Line shows the VF fit of all data for the α-relaxation times.

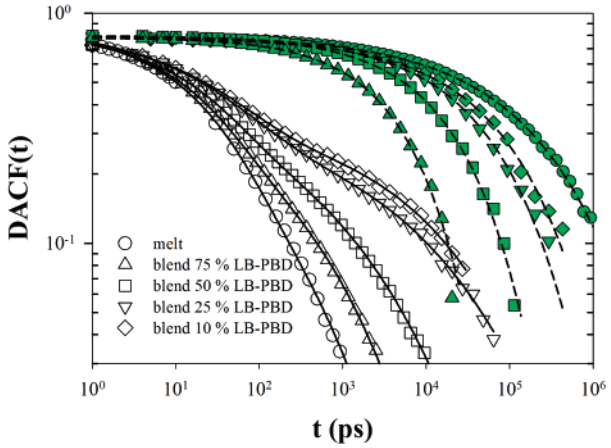

Figure 4. DACF as a function of time for LB-PBD (open symbols) and CR-PBD (filled symbols) components in the LB-PBD/CR-PBD blends and pure melts at 198 K. Lines show fits using eqs 10 and 11 for CR-PBD and LB-PBD components, respectively. Estimated uncertainties are smaller than the symbol size.

dielectric response of CR-PBD melts.[28] Taking this into account, we fit the DACF for the CR-PBD melts using two processes (eq 11) fixing the stretching exponent for the α-relaxation process to experimental value[36] of $\beta = 0.41$ since we do not have simulation data for temperatures below T_g of the CR-PBD that would allow us to independently determine the constant stretching exponent. We found that for $T > 225$ K this fitting protocol provides relaxation times and amplitudes for the α- and β-relaxation processes that are in good agreement with experimental data. The α-relaxation times nicely follow the VF temperature dependence of the experimental data, as shown in Figure 3, while the amplitudes for this process were between 0.08 and 0.15 for the temperature range between 400 and 225 K. The β-relaxation times are also consistent with experiment.

For lower temperatures (225−198 K), constraining $\beta = 0.41$ for the α-relaxation process yields α-relaxation times that are systematically lower than experiment and do not follow the VF behavior observed for MD simulations at higher temperatures. We believe that in this temperature range the α-relaxation is not adequately sampled in our simulations due to very long relaxation times. The DACFs decay only to about 0.4−0.5 on the multiple microsecond time scale of our simulations. Taking into account that the β-relaxation process in this temperature range constitutes the majority of the relaxation,[36] we find that the fits to our DACFs in this temperature range are relatively insensitive to the representation of the α-relaxation. Therefore, in this temperature range, in addition to fixing KWW stretching parameter, we also fixed the relaxation time for the α-relaxation process as obtained from a VF fit of experimental and high temperature simulations data[36] and allowed the amplitudes and parameters for the β-relaxation to be adjustable. This fitting protocol produced relaxation times for the β-process that are in agreement with high-temperature data as well as experimental data, as shown in Figure 3. We also found that the amplitude for the β-relaxation process at the lowest temperature investigated (198 K) was about 0.7, consistent with analysis of experiment.[36] The stretching exponent for the β-relaxation process was found to be between 0.6 and 0.7 over the entire temperature range.

We believe that these findings for pure melts have important consequences for segmental relaxation mechanisms in miscible polymer blends. Since, as discussed above, the α-relaxation process in amorphous polymers depends on cooperative motion of the local environment (matrix) while the β-relaxation process is a local process that depends much less on matrix mobility, we anticipate that blending will influence the α-relaxation process of the component polymers much more than their β-relaxation processes. This effect may be particularly important for the lower T_g component since the β-relaxation process is likely to be comparable in strength to or even stronger than the α-relaxation process at temperatures above the T_g of the pure lower T_g component.

B. Composition Dependence of Dipole Moment Relaxation in LB-PBD/CR-PBD Blends. In Figure 4 we show the DACF of the fast (LB-PBD) and slow (CR-PBD) blend components for several blend compositions at 198 K. Also shown is the DACF for the pure component melts. Signatures of the α- and β-relaxation processes can be clearly seen for the pure LB-PBD melt. As dynamically slow CR-PBD is blended with the fast LB-PBD component, the β-relaxation process of the fast LB-PBD blend component is influenced very little while the α-relaxation process for this component is strongly dependent on blend composition. The DACFs shown in Figure 4 were fitted using eq 11 (two processes) for the LB-PBD component and eq 10 (combined process) for the CR-PBD component. For the LB-PBD component no constraints on the KWW parameters were imposed in the fitting. The α- and β-relaxation processes are well separated in this component, and the fits were consistently converging to the same set of parameters independently of initial values. However, significant overlap of the α-relaxation and β-relaxation processes as well as incomplete sampling of the α-relaxation process within the simulation time window for the CR-PBD component significantly complicates the fitting of DACFs for this component using two relaxation processes (eq 11). Unlike the pure CR-PBD melt, where experiment provides constraints in our fitting, for the blend there is no additional information that would allow us to define such constraints. Therefore, our attempt to fit the CR-PBD response in the blend using two processes (eq 11) resulted in a broad range for some parameters that provided nearly identical descriptions of the data. Consequently, we fit relaxation in the CR-PBD blend component as a combined ($\alpha + \beta$)-relaxation process.

The integrated relaxation times for the α- and β-relaxation processes of the LB-PBD component and ($\alpha + \beta$)-relaxation process of the CR-PBD component are shown in Figure 5a as a function of blend composition. For the LB-PBD component the insensitivity of the β-relaxation time and the strong

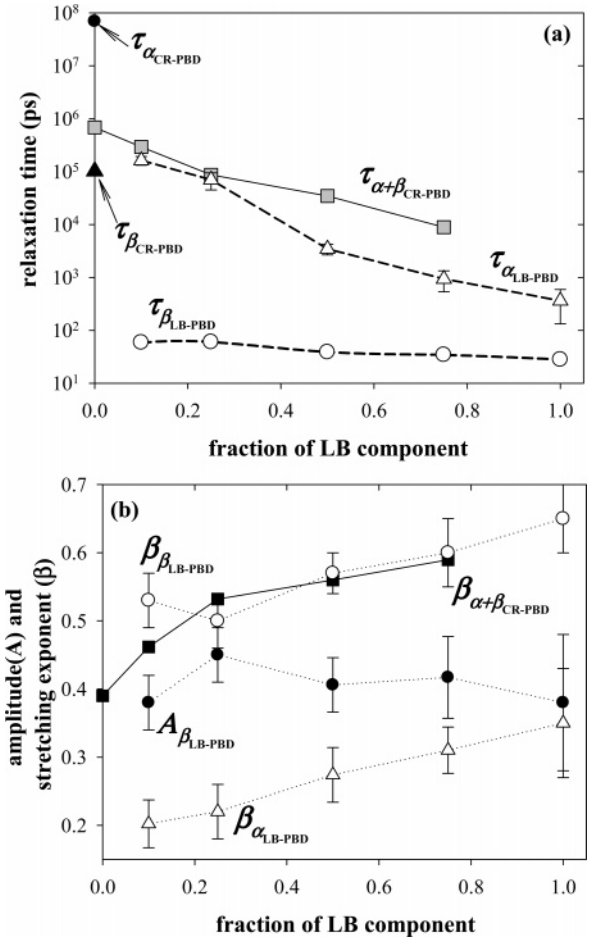

Figure 5. (a) Integrated relaxation times for the α- and β-relaxation processes of LB-PBD and combined (α + β)-relaxation process of the CR-PBD component as a function of blend composition at 198 K. Also shown are the integrated relaxation times for α- and β-relaxation processes in CR-PBD melt. (b) Composition dependence of KWW stretching parameter (β) and amplitudes for the α- and β-relaxation processes of LB-PBD and combined (α + β)-relaxation process of the CR-PBD component. Lines are for eye guidance. The error bars are either less than the symbol size or indicated explicitly.

dependence of the α-relaxation time on blend composition can be clearly seen. For the CR-PBD component the relaxation time for the (α + β)-relaxation process decreases monotonically with increasing fraction of the fast component. For the pure melt of the CR-PBD we also show relaxation times for the α- and β-relaxation processes obtained as described in section IVA. The relaxation time obtained for the combined process lies between relaxation times of α- and β-relaxation processes, as anticipated.

In Figure 5b we show amplitudes and stretching exponents for the KWW functions for each process for both components. The stretching exponent for the β-relaxation process of the LB-PBD component decreases slightly as the concentration of the slow component increases. However, the α-relaxation process in the LB-PBD component broadens significantly with increasing concentration of the slow component. For the CR-PBD component, significant narrowing of the combined (α + β)-relaxation process is observed upon blending with the fast LB-PBD component, particularly for low LB-PBD content blends. This narrowing is likely due to a combination of reduced separation between the α- and β-relaxation processes with blending (note that in the pure melt at 198 K the processes in CR-PBD are separated by almost 3 orders of magnitude, as shown in Figure 5a) and intrinsic narrowing of the individual processes. A similar trend has been observed in the application of CM to glass-forming liquid mixtures.[21,39] The stronger composition dependence of the width of the combined relaxation in the CR-PBD component for low LB-PBD content blends may indicate that while separation of the α- and β-processes is significantly reduced by initial blending, reflecting a greater influence (speeding up) of the α-relaxation than the β-relaxation upon blending with the fast LB-PBD component, further increase in the LB-PBD content has relatively little additional influence on the separation once the separation has been greatly reduced by initial blending.

The amplitude of the β-relaxation process (and hence the α-relaxation as well) of the LB-PBD component shows almost no concentration dependence. The strength of the β-relaxation process in the LB-PBD melt at this temperature (well above T_g of the pure LB-PBD melt) is comparable to the strength of the α-relaxation process. The composition independence of the strength of the LB-PBD component β-relaxation process indicates that the β-relaxation process of the fast component, while becoming well separated from the α-relaxation process upon blending, remains strong for all blend compositions and is responsible for a significant fraction of the relaxation of the fast LB-PBD component in the blend.

The two most salient conclusions from these analyses of dipole moment relaxation in CR-PBD/LB-PBD blends are (1) that the (main chain) β-relaxation process of the fast component is insensitive to blending at temperatures that are well above glass transition of this component and (2) that the α-relaxation process of the fast component broadens significantly upon blending. Insensitivity of subglass relaxation processes to blending has been observed experimentally.[23,40] However, these observations were made for blends where the subglass process is associated with side group motion and at temperatures below the glass transition where the segmental and subglass processes are well separated. Broadening of segmental relaxation of the dynamically fast component has been observed in many polymer blends and is predicted by CF models.[4,12,23] However, we do not believe that concentration fluctuations play a dominant role in determining the dielectric response of CR-PBD/LB-PBD blends. According to CF models, the concentration fluctuations should become negligible in dilute mixtures, and therefore no broadening of component relaxation can be expected in this concentration regime. We observe monotonically increased broadening of the response of the LB-PBD component with increasing concentration of the CR-PBD component even in relatively dilute (in the LB-PBD component) blends. Furthermore, the combined (α + β)-relaxation process in the CR-PBD component of the LB-PBD/CR-PBD blends appears to *narrow* upon blending with LB-PBD, counter to the predictions of the CF models.

It has been claimed that the CM predicts both insensitivity of the β-relaxation of the fast blend component to blending and broadening of the α-relaxation process of the fast blend component with increasing concentration of the slow component.[22] We investigated the applicability of the CM to the relaxation behavior of the LB-PBD component in our CR-PBD/LB-PBD blends. Note that all parameters of eq 7 (except t_c) are available from the fits of LB-PBD DACF at any composition, and their compliance with eq 7 can be easily evaluated. We used τ_α^{KWW} and τ_β^{KWW} from our KWW fits of the DACF and calculated $\beta_\alpha = 1 - n$ using the CM with t_c = 2 ps. The predicted values of β_α are shown in Figure 6. The CM prediction for β_α for the LB-PBD component of the CR-PBD/LB-PBD blends is qualitatively different from that observed in our simulations. The predicted relaxation is much

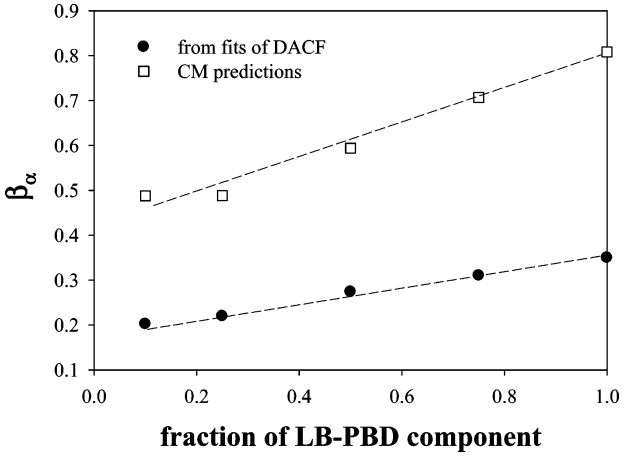

Figure 6. Composition dependence of the KWW stretching parameter for the α-relaxation process of the LB-PBD component as obtained from fitting the DACFs and from prediction using CM.

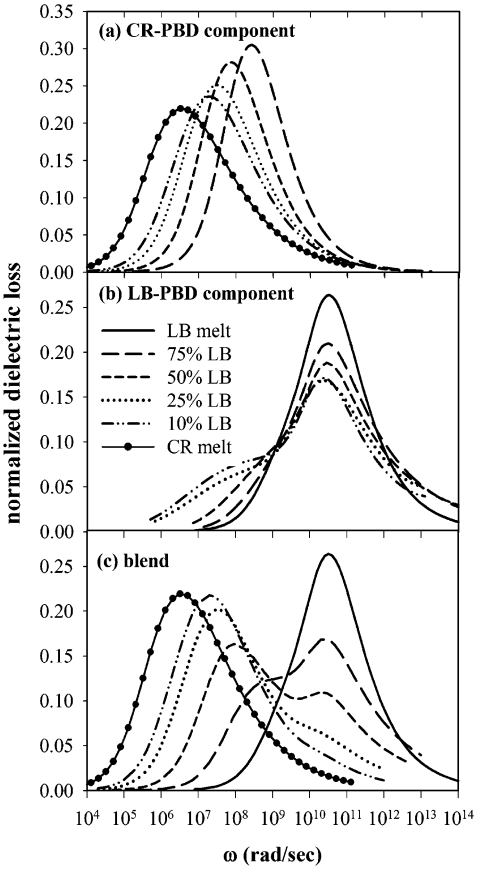

Figure 7. Normalized dielectric loss of (a) the CR-PBD component, (b) the LB-PBD component, and (c) the LB-PBD/CR-PBD blend at 198 K for several blend compositions and pure melts of the components. All curves are normalized such that the total dielectric loss is unity.

narrower than that observed in our simulations. The CM predicted response of the LB-PBD component in the blend with the lowest LB-PBD concentration is narrower than observed in the pure LB-PBD melt.

C. Composition Dependence of Dielectric Loss in LB-PBD/CR-PBD Blends. Using eq 6, we have calculated the dielectric response of the LB-PBD/CR-PBD blends and individual components in the blends, as shown in Figure 7. For the CR-PBD component (Figure 7a) the dielectric loss becomes narrower and shifts to higher frequencies upon blending, consistent with a decrease in relaxation times and with either narrowing of the relaxation processes or reduced separation between the α- and

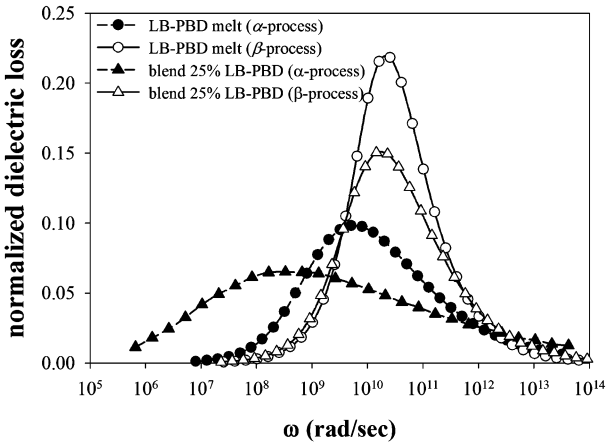

Figure 8. Contributions due to α- and β-relaxation processes to the dielectric loss of LB-PBD in the pure melt and the 25/75 LB-PBD/CR-PBD blend at 198 K. Contribution for each process has been scaled proportionally to the corresponding amplitudes (A_α and A_β) obtained from fitting the DACFs and renormalized such that the sum of the α- and β-relaxation process gives unity dielectric loss for each case. Contributions in the blends were not weighted by the blend composition.

β-relaxation processes (as discussed above) for the slow CR-PBD component with increasing concentration of the fast LB-PBD component. The dielectric response of the LB-PBD component (Figure 7b) shows the development of a low-frequency shoulder as the concentration of the slow CR-PBD component increases, consistent with the increasing separation between the α- and β-relaxation processes observed in the DACFs. In Figure 7c, we show the normalized total dielectric loss of the LB-PBD/CR-PBD blends as a function of frequency. The total dielectric response of the blend consists of two clear peaks: (1) a broad low-frequency peak due to relaxation of the CR-PBD component (combined ($\alpha + \beta$)-relaxation process) shifted to higher frequency compared to the CR-PBD pure melt combined with the α-relaxation process of the LB-PBD component shifted to lower frequency compared to the LB-PBD pure melt and (2) a high-frequency peak due to primarily the β-relaxation process of the LB-PBD component (uninfluenced by blending) and the high-frequency tails of the α-relaxation process of the LB-PBD component and the combined ($\alpha + \beta$)-relaxation process of the CR-PBD component. The striking similarity of features in the blend dielectric loss observed for the 50/50 PI/PVE and 50/50 LB-PBD/CR-PBD blends (Figure 1, a and b) allows us to conclude that the relaxation mechanism responsible for the high-frequency peak in the blend response is similar for the two blends.[41]

Decomposition of the dielectric response of the LB-PBD component into contributions from the α- and β-relaxation processes is shown in Figure 8 for one blend composition and is compared with the dielectric susceptibility of the corresponding pure melt. As expected, the dielectric loss due to the β-relaxation process of the LB-PBD component does not shift in frequency or strength upon blending,[42] while the contribution due to the α-relaxation process shifts to lower frequencies, broadens, and overlaps with the response of the CR-PBD component.

D. Temperature Dependence of Dipole Moment Relaxation in LB-PBD/CR-PBD Blends. In Figure 9 we show the DACFs and their fits with eqs 11 and 10 for the LB-PBD and CR-PBD components, respectively, as a function of temperature in the blend with 10% LB-PBD. For both components we have applied the same fitting procedure as in the analysis of the composition dependence described above. The temperature

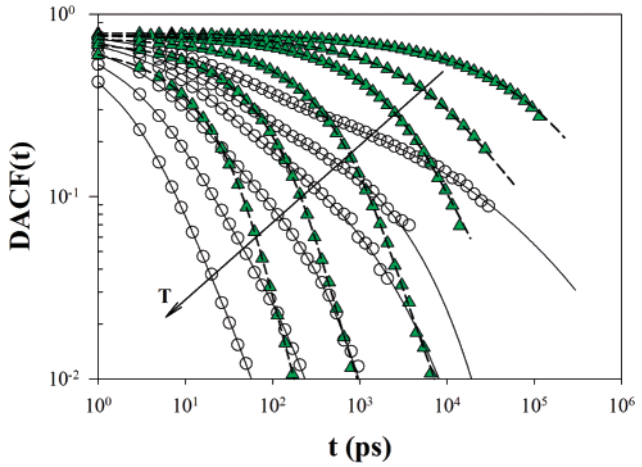

Figure 9. DACF as a function of time for LB-PBD (open symbols) and CR-PBD (filled symbols) components in the 10/90 LB-PBD/CR-PBD blends at 198, 222, 240, 273, 323, and 400 K. Lines show fits using eqs 10 and 11 for CR-PBD and LB-PBD components, respectively. Arrow indicates the direction of increasing temperature. Uncertainties are smaller than the symbol size.

dependence of the integrated relaxation times for the LB-PBD β-relaxation process is illustrated in Figure 10a, while integrated relaxation times for the α-relaxation process of the components in the pure melts, the LB-PBD α-relaxation process in the blend, and the combined CR-PBD (α + β)-relaxation process in the blend are shown in Figure 10b for the 10% LB-PBD blend and in Figure 10c for the 50% LB-PBD blend.

Figure 10a clearly shows that the temperature dependence of the β-relaxation processes for the LB-PBD component in the blends is very similar to that in pure melt of this component due to the insensitivity of the β-relaxation process to blending with the slow CR-PBD as discussed extensively above. The β-relaxation times for LB-PBD can be well described by an Arrhenius temperature dependence in both the pure melt and the 10% and 50% LB-PBD blends. The α-relaxation process of the LB-PBD component in the blends shown in Figure 10b,c exhibits significantly stronger temperature dependence than the pure LB-PBD melt over the range of temperatures studied. However, even in the 10% LB-PBD blend despite the dominance of the slow component (90%) in the blend, the α-relaxation process for the LB-PBD component is faster than the dominant CR-PBD component (combined (α + β)-relaxation process). The relaxation times for the combined (α + β)-relaxation process of the CR-PBD component have relatively weak temperature dependence that seems eventually to cross over the temperature dependence of the LB-PBD α-relaxation process. This "unphysical" behavior is due to fitting the contributions of both α- and β-relaxation processes that have quite different temperature dependences and magnitudes of characteristic relaxation times using one KWW function. The separation between the (α + β)-relaxation processes increases with decreasing temperature, and it becomes more difficult to adequately/completely sample the contribution of the α-process to relaxation due to increasing α-relaxation times. As a consequence, the relaxation time obtained for the combined (α + β)-relaxation process deviates more from the true segmental (α-) relaxation time with decreasing temperature. Unfortunately, similar problems might be emerging in interpretation of experimental data using techniques that are limited to relatively fast observation times (e.g., spin−lattice NMR and QENS) and therefore, as in our simulations, cannot differentiate contributions of secondary and primary relaxation processes and therefore

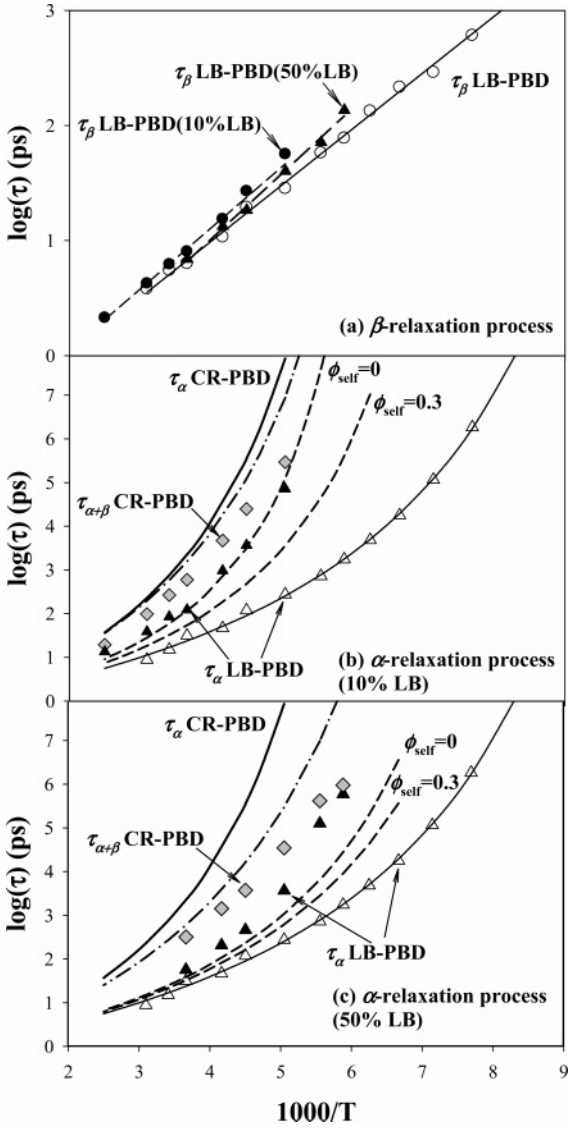

Figure 10. Integrated relaxation times for the α- and β-relaxation processes of LB-PBD and CR-PBD components as a function of inverse temperature for the LB-PBD/CR-PBD blend and pure melts. (a) Relaxation times for the β-relaxation processes. The error bars are comparable to the symbol size. Lines show Arrhenius fits (eq 13). (b, c) Relaxation times for the α-relaxation processes (LB-PBD) and combined (α + β)-relaxation process (CR-PBD) in 10% and 50% LB-PBD blend, respectively. Solid lines show the VF fit of components pure melt data, dashed lines show the LM model prediction for the LB-PBD α-relaxation process with ϕ_{self} = 0.3 and 0.0, and dashed-dotted lines show the LM prediction for the CR-PBD component in the blend with ϕ_{self} = 0.3.

provide an unexpectedly weak temperature dependence of component segmental relaxations in some blends.

To investigate the applicability of the "self-concentration" concept of the LM model to segmental relaxation in our LB-PBD/CR-PBD blends, we have attempted to represent the segmental relaxation times and their temperature dependence for the α-relaxation processes in the 10% and 50% LB-PBD blends using the LM model. The VF fits to the dipole moment autocorrelation times for the pure melts were extrapolated to low temperatures, and the temperature where the segmental relaxation time reached 1 s was considered T_g for the corresponding polymer melt (CR-PBD T_g = 164 K, LB-PBD T_g = 108 K). We then calculated $T_{g,eff}$ for each component in the blend (ϕ = 0.1 and 0.5 of the LB-PBD component) using the Fox equation (eq 2) where ϕ_{eff} has been determined using ϕ_{self} =

0.3 estimated for PBD.[11] Finally, the segmental relaxation times from the LM model for each blend component have been predicted using eq 3 where the τ_∞^i and B^i parameters for i = {CR-PBD, LB-PBD} were kept the same as for corresponding pure melts while T_0^i were determined using eq 4. In Figure 10b,c we show predictions by the LM model for the α-relaxation times of the LB-PBD and CR-PBD components with ϕ_{self} = 0.3. The LM predictions for the segmental relaxation times for the CR-PBD component deviate significantly from the relaxation times of the combined (α + β)-relaxation process observed in the blend. This deviation increases with decreasing temperatures due to weaker temperature dependence of the combined (α + β)-relaxation process than can be expected from the true α-relaxation process. It is possible that deviation between LM predictions for the segmental relaxation time of blend components and observed relaxation times (experimental or simulation) in some blends may be due, at least in part, to the inability of the measuring technique to separate strong local β-relaxation contributions to the relaxation from the true segmental relaxation process (the α-process) and/or a measurement window that does not allow sufficient sampling of the long-time contribution of the α-process to segmental relaxation.

For the LB-PBD blend component, where it is possible to separate relaxation due to the local and segmental processes and to completely sample the α-relaxation, it is clear that the LM model with ϕ_{self} = 0.3 significantly underestimates the slowing down of segmental relaxation upon blending for both compositions. Hence, the LM model with a physically reasonable ϕ_{self} underestimates the coupling between segmental dynamics of the LB-PBD component and the dynamics of the matrix. The ϕ_{self} = 0.0 for the LB-PBD component provides a better description of the α-relaxation times for the LB-PBD component in the 10% LB-PBD blend, as illustrated in Figure 10b, indicating that, within the LM formulation, the segmental relaxation of the fast component is determined entirely by the bulk composition of the blend which is contrary to the spirit of the LM model which assumes that the local, dynamically relevant environment for a segment differs in composition from the bulk blend due to chain connectivity effects. However, in the 50% LB-PBD (Figure 10c), even with ϕ_{self} = 0.0, the LM underestimates the slowing down of the α-relaxation of the LB-PBD component.

The inability of the LM model to predict segmental relaxation times for the LB-PBD component in the LB-PBD/CR-PBD blends illustrates that the segmental relaxation processes for the blend components cannot be understood in terms of segmental dynamics of the pure melts combined with a temperature-independent local environment that exhibits an effective glass transition temperature. Specifically, the segmental dynamics of the fast LB-PBD component appear to be too strongly coupled to the dynamics of the matrix than allowed within such a simple framework, as illustrated in Figure 10b,c. A Vogel−Fulcher fit (eq 3) of the α-relaxation times for the minority LB-PBD component in the 10% LB-PBD blend yields a T_0 value quite similar to that found for the CR-PBD melt. This correspondence seems to indicate an increasing dominance of the CR-PBD dominated matrix in determining the segmental relaxation behavior for the minority LB-PBD with decreasing temperature.

V. Conclusions

The above analyses of segmental relaxation processes in LB-PBD/CR-PBD blends allow us to make several important observations regarding relaxation mechanisms in miscible polymer blends. First, we observe that blending with a significantly slower component promotes separation between the α- and β-relaxation processes of the fast component. Second, the relaxation time for the β-relaxation process of the fast component is at most weakly affected by blending while the α-relaxation time of the fast component exhibits strong concentration dependence. Third, the β-relaxation process in the fast component preserves its strength upon blending and can be comparable in strength to the α-relaxation process at temperatures well above T_g of the fast component pure melt. In fact, we find that the β-relaxation process of the fast component constitutes the majority of the blend dielectric loss at high frequency. The dielectric response due to the α-relaxation process of the LB-PBD component broadens significantly, shifts to lower frequencies, and overlaps with the response ((α + β)-relaxation process) of the slow component (CR-PBD) upon blending. For the CR-PBD component, the overall dielectric response becomes narrower upon blending with the fast (LB-PBD) component. This seems to be a combination of two effects: (a) slight narrowing of the relaxation processes and (b) decrease in separation between α- and β-relaxation processes.

The dielectric response obtained from our MD simulations of LB-PBD/CR-PBD blends is qualitatively similar to the experimental dielectric response of real polymer blends comprised of dielectrically active component polymers with significantly different segmental dynamics. We interpret the high-frequency loss observed in numerous dielectric spectroscopy studies of miscible polymer blends that is apparently uninfluenced by blending as being due to the intrinsic β-relaxation process (secondary relaxation, intramolecular in nature) of backbone dihedrals of the fast component and not due to concentration fluctuations and/or structural heterogeneities within the blend. In other words, instead of assuming that some fraction of the fast component is not affected upon blending due to the presence of the pure meltlike local environments, we believe that a *fraction of the local intramolecular backbone relaxation* of the fast component (the β-relaxation process) is not (or only slightly) affected by blending and contributes *homogeneously* to the high-frequency response of the blend, while the contribution from the α-relaxation process is shifted to lower frequencies with increasing fraction of the slow component.

Finally, we note that when techniques such as NMR spin−lattice relaxation or QENS are employed in the study of the dynamics of miscible polymer blends, measurements are often made at temperatures that are well above the glass transition temperature of the fast component. This is required to move the segmental relaxation time of the fast component into the experimental time window. At these temperatures, the β-relaxation process can dominate the merged or nearly merged segmental relaxation.[23,43] We speculate, therefore, that NMR spin−lattice and QENS measurements may be primarily sensitive to the β-relaxation process of the fast component relaxation in some blends and may not detect, or only partially detect, contributions from the composition-dependent α-relaxation of the fast component that may be fairly weak at temperatures well above the T_g of the fast component. As a result, these techniques may yield an anomalously weak (apparent) composition dependence of the segmental relaxation time for the fast component on blend composition by associating the segmental relaxation time with the relatively matrix-insensitive β-relaxation process and not the composition-dependent α-relaxation process of the fast component.

Acknowledgment. The authors thank Professor Mark Ediger and Professor Wolfgang Paul for helpful discussions as well as

acknowledge the support by the Center for the Simulation of Accidental Fires and Explosions (C-SAFE) funded by the Department of Energy, Lawrence Livermore National Laboratory, under Subcontract B341493.

References and Notes

(1) *Polymer Blends Handbook*; Utracki, L. A., Ed.; Kluwer Academic Publishers: Boston, 2002.
(2) Zetsche, A.; Fischer, E. W. *Acta Polym.* **1994**, *45*, 168.
(3) Lodge T. P.; McLeish, T. C. B. *Macromolecules* **2000**, *33*, 5278.
(4) Kamath, S.; Colby, R. H.; Kumar, S. K.; Karatasos, K.; Floudas, G.; Fytas, G. *J. Chem. Phys.* **1999**, *111*, 6121.
(5) Chung, G.-C.; Kornfield, J. A.; Smith, S. D. *Macromolecules* **1994**, *27*, 964. Chung, G.-C.; Kornfield, J. A.; Smith, S. D. *Macromolecules* **1994**, *27*, 5729.
(6) Colby, R. H.; Lipson, J. E. *Macromolecules* **2005**, *38*, 4919.
(7) Fox, T. G. *Bull. Am. Phys. Soc.* **1956**, *1*, 123.
(8) Vogel, H. *Phys. Z.* **1921**, *22*, 645.
(9) Fulcher, G. S. *J. Am. Chem. Soc.* **1925**, *8*, 339.
(10) Adams, G.; Gibbs, J. H. *J. Chem. Phys.* **1965**, *43*, 139.
(11) He, Y.; Lutz, T. R.; Ediger, M. D. *J. Chem. Phys.* **2003**, *119*, 9956.
(12) Leroy, E.; Alegria, A.; Colmenero, J. *Macromolecules* **2003**, *36*, 7280.
(13) Lutz, T. R.; He, Y.; Ediger, M. D.; Cao, H.; Lin, G.; Jones, A. A. *Macromolecules* **2003**, *36*, 1724.
(14) Urakawa, O.; Sugihara, T.; Adachi, K. *Polym. Appl.* (*Jpn.*) **2002**, *51*, 10.
(15) Lorthoir, C.; Alegria, A.; Colmenero, J. *Phys. Rev. E* **2003**, *60*, 031805.
(16) Roland, C. M.; Ngai, K. L. *Macromolecules* **1991**, *24*, 2261. Roland, C. M.; Ngai, K. L. *Macromolecules* **1992**, *25*, 363. Roland, C. M.; Ngai, K. L. *Macromolecules* **2000**, *33*, 3184.
(17) Colmenero, J.; Arbe, A.; Goddens, G.; Frick, B.; Mijangos, C.; Reinecke, H. *Phys. Rev. Lett.* **1997**, *78*, 1928.
(18) Kohlrausch, F. *Poggendorff's Ann. Phys.* **1863**, *119*, 352.
(19) Williams, G.; Watts, D. C. *Trans. Faraday Soc.* **1970**, *66*, 80.
(20) Capaccioli, S.; Ngai, K. L. *J. Phys. Chem. B* **2005**, *109*, 9727.
(21) Ngai, K. L.; Capaccioli, S. *J. Phys. Chem. B* **2004**, *108*, 11118.
(22) Ngai, K. L.; Roland, C. M. *Macromolecules* **2004**, *37*, 2817. Ngai, K. L.; Roland, C. M. *Rubber Chem. Technol.* **2004**, *77*, 579.
(23) Arbe, A.; Alegria, A.; Colmenero, J.; Hoffmann, S.; Willner, L.; Richter, D. *Macromolecules* **1999**, *32*, 7572.
(24) Bedrov, D.; Smith, G. D. *Macromolecules* **2005**, *38*, 10314.
(25) Smith, G. D.; Paul, W. *J. Phys. Chem. A* **1998**, *102*, 1200.
(26) Smith, G. D.; Borodin, O.; Bedrov, D.; Paul, W.; Qiu, X. H.; Ediger, M. D. *Macromolecules* **2001**, *34*, 5192.
(27) Smith, G. D.; Paul, W.; Monkenbusch, M.; Richter, D. *Chem. Phys.* **2000**, *261*, 61. Smith, G. D.; Paul, W.; Monkenbusch, M.; Richter, D. *J. Chem. Phys.* **2001**, *114*, 4285.
(28) Smith, G. D.; Borodin, O.; Paul, W. *J. Chem. Phys.* **2002**, *117*, 10350.
(29) Krushev, S.; Paul, W.; Smith, G. D. *Macromolecules* **2002**, *35*, 4198.
(30) Smith, G. D.; Bedrov, D. *J. Non.-Cryst. Solids*, in press.
(31) Ryckaert, J.; Ciccotti, G.; Berendsen, H. J. C. *J. Comput. Phys.* **1977**, *23*, 327.
(32) Edwards, D. M. F.; Madden, P. A.; McDonald, I. R. *Mol. Phys.* **1984**, *51*, 1141.
(33) Smith, G. D.; Paul, W.; Monkenbusch, M.; Willner, L.; Richter, D.; Qiu, X. H.; Ediger, M. D. *Macromolecules* **1999**, *32*, 8857.
(34) Boyd, R. H.; Smith, G. D. *Polymer Relaxation and Dynamics*; Cambridge University Press: New York, in press.
(35) Ngai, K. L.; Paluch, M. *J. Chem. Phys.* **2004**, *120*, 857.
(36) Arbe, A.; Richter, D.; Colmenero, J.; Farago, B. *Phys. Rev. E* **1996**, *54*, 3853.
(37) Arbe, A.; Colmenero, J.; Gomez, D.; Farago, B.; Richter, D. *Phys. Rev. E* **1999**, *60*, 1103.
(38) Smith G. D.; Bedrov, D.; Paul, W. *J. Chem. Phys.* **2004**, *121*, 4961.
(39) Psurek, T.; Maslanka, S.; Paluch, M.; Nozaki, R.; Nhai, K. L. *Phys. Rev. E* **2004**, *70*, 011503.
(40) Cendoya, I.; Alegria, A.; Alberdi, J. M.; Colmenero, J.; Grimm, H.; Richter, D.; Frick, B. *Macromolecules* **1999**, *32*, 4065.
(41) Smith, G. D.; Bedrov, D. *Eur. Polym. J.*, in press.
(42) Differences in the maximum loss for the β-relaxation in the LB-PBD blend component for different blend compositions are due to differences in the width of the process and not due to differences in the strength of the process.
(43) Bedrov, D.; Smith, G. D. *Phys. Rev. E* **2005**, *71*, 050801(R).

MA0608828